ECRONICON OPEN ACCESS

EC ORTHOPAEDICS
Research Article

Bone Marrow-Derived Mesenchymal Stem Cells Reduce Glycosaminoglycan Deposition in Deep Digital Flexor Collagenase-Induced Tendinopathy

Sherry A Johnson[1], John D Lutter[2], Robert K Schneider[3], Elizabeth W Biscoe[4], Gregory D Roberts[5], Julie A Cary[5] and David D Frisbie[1]*

[1]*Department of Clinical Sciences, Orthopaedic Research Center at the C. Wayne McIlwraith Translational Medicine Institute, College of Veterinary Medicine and Biomedical Sciences, Colorado State University, Fort Collins, CO, USA*

[2]*Kansas State University, Veterinary Health Center, Manhattan, KS, United States*

[3]*Schneider and Stenslie Equine, Auburn, WA, USA*

[4]*Animal Imaging, Irving, TX, USA*

[5]*Department of Veterinary Clinical Sciences, College of Veterinary Medicine, Washington State University, Pullman, WA, United States*

***Corresponding Author:** David D Frisbie, Department of Clinical Sciences, Orthopaedic Research Center at the C. Wayne McIlwraith Translational Medicine Institute, College of Veterinary Medicine and Biomedical Sciences, Colorado State University, Fort Collins, CO, USA.

Received: May 13, 2021; **Published:** June 08, 2021

Abstract

Intrathecal deep digital flexor tendon (DDFT) injuries are a common source of distal limb lameness in athletic horses with prognosis considered guarded to poor. The ability of mesenchymal stem cells to improve intrathecal DDFT healing is difficult to objectively evaluate in the clinical setting due to inherent variations in extent, severity, configuration and chronicity of naturally occurring lesions. The study objective was to evaluate the effects of intra-lesional mesenchymal stem cells compared to untreated controls in a collagenase model of intrathecal deep digital flexor tendinopathy. Tendinopathy of both forelimb DDFTs within the pastern region was induced with collagenase. One randomly assigned limb was treated with intra-lesional MSC injection with the opposite limb serving as untreated control. Horses were placed into a controlled exercise program with ultrasonographic and magnetic resonance imaging evaluations at 0, 14-, 60-, 90-, and 214-days post treatment. Post-mortem histologic and biochemical analysis was performed. Inflammatory cellular infiltration and glycosaminoglycan content were significantly lower in MSC treated tendons (P = .05, P = .002, respectively). The results herein demonstrate that the use of MSCs significantly lessened the amount of inflammatory cellular infiltrate and glycosaminoglycan content in enzymatically damaged intrathecal DDF tendon cells (130% and 42% reductions, respectively). Only subtle differences in ultrasonographic or MRI imaging characteristics were appreciated, leading authors to speculate that physiologic effects of MSCs may not manifest as imaging-apparent differences. The use of MSCs in collagenase induced DDF tendinopathy is associated with chronic tendon enlargement, improved glycosaminoglycan content and a decreased inflammatory response.

Keywords: *Tendinopathy; Horse; Collagenase*

Introduction

Intrathecal deep digital flexor tendon (DDFT) injuries are a common source of distal limb lameness in athletic horses, being documented in 83% of cases evaluated with high-field magnetic resonance imaging (MRI) [1]. The physiologic complexity of distal limb DDFT

injuries has been attributed to structural and biomechanical differences that occur in the proximal to distal and dorsal to palmar directions, with 50% of lesions occurring within the pastern region [2] and 96% of those configured as core lesions [2]. Prognosis for athletic soundness in horses with distal limb DDFT injuries is considered guarded to poor, with only 41% of horses with core lesions returning to some level of activity [3]. Therapies capable of improving tendinopathic healing at the cellular level are needed.

Mesenchymal stem cells (MSCs) for use in superficial digital flexor tendon (SDFT) injury have demonstrated beneficial effects in naturally occurring disease [4,5] and various models of tendinopathy [6,7]. The investigation of MSCs and their ability to mitigate intrathecal DDFT injury, however, is difficult to objectively evaluate in the clinical setting due to inherent variations in extent, severity, configuration and chronicity of naturally occurring lesions. Experimental replication of spontaneous tendon injury is difficult, but collagenase (enzymatic) models have demonstrated characteristics consistent with clinical disease [8], and the intrathecal DDFT within the pastern region lends itself to non-invasive anatomic access.

Objective of the Study

Therefore, the objective of this study was to evaluate the effects of intra-lesional MSCs compared to untreated controls in a collagenase model of intrathecal deep digital flexor (DDF) tendinopathy.

Materials and Methods

This study was a prospective, blinded experiment. All study methods were conducted in compliance with Washington State University's Institutional Animal Care and Use Committee (IACUC) standards (protocol #4207).

Experimental animals

The experimental sample size (six limbs) was calculated using GPower Version 3.1.1 (GPower, Brunsbuttel Germany). Values from a published study investigating glycosaminoglycan content of stem cell intra-lesional therapy over six months were used for power calculation [4]. Specifically, an a priori power analysis was conducted. Using a two-sample t-test with expected group mean difference of 18, this power analysis resulted in an effect size of 2.571 and a power of 0.95 using a 95% confidence interval and a standard deviation of 8 µg/mg glycosaminoglycan content between groups. Six adult horses of various breeds (two American Quarter Horses, one American Paint Horse and three Arabians), ages two to eight years purchased from an outside vendor that showed no clinical or magnetic resonance imaging evidence of current or previous forelimb DDFT injury were enrolled. The enrolled study population consisted of 3 mares and 3 geldings.

Tendinopathy induction and post-operative care

All horses were pre-medicated with xylazine hydrochloride (1.1 mg/kg IV) and butorphanol tartrate (0.05 mg/kg IV) prior to being placed under anesthesia using diazepam (0.05 mg/kg IV) and ketamine hydrochloride (2.2 mg/kg IV). General anesthesia was then maintained with inhaled isoflurane for the duration of the procedure during which DDF tendinopathy was induced using ultrasound guidance in a manner similar to that previously described [9]. Briefly, 500 units of filter-sterilized bacterial collagenase (c0130 Sigma Aldrich Co., St. Louis, MO) diluted in 0.1 mL of sterile water was injected into the medial lobe of both forelimb DDFTs at the level of the proximal interphalangeal joint using a 22' x 1.5" spinal needle. Additional doses of xylazine hydrochloride (0.5 - 1 mg/kg IV), butorphanol tartrate (0.05 mg/kg IV), or ketamine hydrochloride (0.5 - 2.2 mg/kg) were administered to effect before, during, and after the collagenase injection, in accordance with current clinical practices to maintain adequate anesthetic depth. Following injections, both forelimbs were bandaged routinely for 24 hours and all horses were administered two grams of phenylbutazone (4.4 mg/kg) orally every 24 hours for three days. All horses' vital parameters were monitored hourly for three days following collagenase injection.

Following collagenase injection, horses were housed in stalls (4m x 4m) for 28 days, transitioned to 9m x 9m paddocks until 90 days, then housed in a pasture until day 214. Horses were incrementally hand-walked twice daily beginning 14 days after tendinopathy induction (5 minutes twice/day for two weeks, then 10 minutes twice/day for four weeks, lastly 20 minutes twice/day for four weeks). Hand-walking was discontinued when pasture turnout was commenced.

Mesenchymal stem cell harvest, processing and injection

Prior to surgical DDFT lesion induction, bone marrow was harvested from each horse with subsequent processing performed at Advanced Regenerative Therapies (Fort Collins, CO). Colony-forming cultures were developed using low glucose Dulbecco's Modified Eagle's Medium (DMEM, Thermo Fisher Scientific, Waltham, MA) with 10% fetal bovine serum (FBS, Atlas Biologicals, Fort Collins, CO). Mesenchymal stem cell colony-forming units were reseeded at 1.5 x 10^4 cells/cm^2 in minimum essential media (AMEM, Thermo-Fisher Scientific, Waltham, MA) with 10% FBS and 2 ng/ml fibroblastic growth factor-2 (FGF2, Peprotech, Rocky Hill, NJ), then culture-expanded through eight population doublings to ~80% confluence. Culture-expanded MSCs were cryopreserved in 95% autologous serum plus 5% dimethyl sulfoxide.

Forelimbs in this study were then randomized into two treatment groups via coin flip. One randomly assigned forelimb (n = 6 forelimbs) received an intra-lesional MSC injection, while the opposite forelimb of each horse served as an untreated control (n = 6 forelimbs). Specifically, 10x10^6 MSCs suspended in 1mL of 95% autologous serum plus 5% dimethyl sulfoxide were injected as 0.2mL aliquots at five sites approximately every 10mm under ultrasound guidance 14 days following lesion induction. Following MSC injection, the injected forelimbs were bandaged routinely for 24 hours. Limbs in Group 2 (n = 6 forelimbs, controls) did not receive any form of intra-lesional injection.

Magnetic resonance image acquisition and analysis

Two-dimensional magnetic resonance (MR) transverse and sagittal plane images (3.5 - 4 mm, no gap) were acquired for both forelimbs at all imaging time points (Figure 1, days 0, 14, 60, 90 and 214) with a 1.0 Tesla MRI Unit (Gyroscan, Philips Healthcare, Best, Netherlands). Sequences obtained included proton density turbo spin echo (PD TSE), T2-weighted TSE (T2 TSE) and short τ inversion recovery (STIR). All images were acquired from the level of the proximal sesamoid bones distally using a 14-15 cm field of view. All MRI studies were performed under general anesthesia except for the day 214 examination which was performed post-mortem. Specific MRI sequence parameters are listed in table 1.

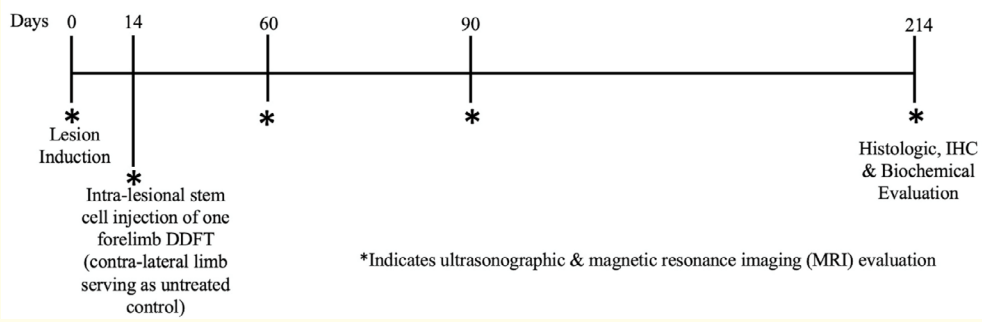

Figure 1: *Experimental timeline, beginning with lesion induction (day 0) and ending with study termination 214 days later. Baseline ultrasonographic and magnetic resonance imaging evaluations were performed prior to lesion induction. Serial imaging evaluations were performed at four time points post lesion creation (days 14, 60, 90 and 214), followed by end point data collection of histologic, immunohistochemical (IHC) and biochemical outcome parameters.*

Image Plane	Sequence	TR (ms)	TE (ms)	FOV (cm)	RFOV (cm)	Matrix	Slice Number	Slice Thickness (mm)	Gap (mm)
Transverse	T2 TSE	2116	100	15	10.5	256 x 512	30	4	0.5
Transverse	PD TSE	2116	11	15	10.5	256 x 512	30	4	0.5
Transverse	STIR	1725	35	15	10.5	192 x 256	30	3.5	1
Sagittal	T2 TSE	3395	110	14	10	256 x 512	22	4	0.5
Sagittal	PD TSE	3395	14	14	10	256 x 512	22	4	0.5
Sagittal	STIR	1500	35	14	10	192 x 256	22	3.5	0.5

Table 1: *Table summarizing the magnetic resonance imaging (MRI) sequence parameters used for imaging of the equine pastern region with the 1.0 Tesla at Washington State University.*

TSE: Turbo Spin Echo; T2: T2 Weighted Sequence; PD: Proton Density; STIR: Short Tau Inversion Recovery; TR: Radiofrequency Pulse Repetition Time; TE: Echo Sampling Time; FOV: Field of View; RFOV: Rectangular Field of View; ms: Microseconds; cm: Centimeter; mm: Millimeter.

Image analysis was performed on a diagnostic imaging viewing station monitor; windowing and leveling was performed to optimize observation of the lesions. All MR images were analyzed by a resident in Equine Surgery (JDL) under the guidance and validation of a board-certified veterinary radiologist (GDR), both blinded to treatment groups. All limbs were randomized for evaluation.

Quantitative measurements for four MRI outcome parameters were made from transverse DICOM images for all obtained sequences using a public domain image program (Image J, U.S. National Institutes of Health, Bethesda, MD). The four MRI outcome parameters considered were 1) mean tendon lobe volume; 2) mean lesion volume; 3) mean tendon lobe signal intensity and 4) mean lesion signal intensity. All collected outcome measures are listed in table 2.

	Grading Criteria	Unit of Measurement or Scale
Ultrasound	Lesion cross-sectional area Tendon cross-sectional area Lesion echogenicity (transverse) Longitudinal fiber pattern	mm^2 mm^2 1 = Isoechoic 2 = Mildly hypoechoic 3 = Moderately hypoechoic 4 = Anechoic 1 = 0 - 25% abnormal 2 = 26 - 50% abnormal 3 = 51 - 75% abnormal 4 = 76 - 100% abnormal
Magnetic Resonance Imaging	Mean lesion volume Mean tendon lobe volume Mean lesion signal intensity Mean tendon lobe signal intensity	mm^2 mm^2 Mean grey value ratio Mean grey value ratio
Cellular Morphology	Cell Shape, Cell Density, Hemorrhage, Neovascularization, Inflammatory Cellular Infiltrate	1 = Normal 2 = Slight 3 = Moderate 4 = Marked

Collagen	Linearity	1 = Linear 2 = > 50% linear 3 = 20% to 50% linear 4 = No linear areas
	Uniformity	1= Uniform diameter of all fibers 2= >50% of fibers are uniform 3 = 20% to 50% of fibers are uniform 4 = Complete disarray of fibers
	Crimping	1 = Coarse, even crimp 2 = Predominantly fine, even crimp 3 = <50% with crimp formation 4 = No crimp formation; complete disarray
Epitenon	Thickness	1 = 1 to 2 cells (normal) 2 = 3 to 6 cells 3 = 7 to 15 cells 4 = Massive fibrosis
Toluidine Blue	Amount of Uptake	0= None 1= Slight 2= Moderate 3= Normal
Collagen Type I	Presence of Type I Collagen	1 = > 90% type I 2 = > 50% to 90% type I 3 = 10% to 50% type I 4 = <10% type I
Collagen Type III	Presence of Type III Collagen	1 = <10% type III 2 = 10% to 50% type III 3 = > 50% to 90% type III 4 = > 90% type III
Aggrecan	Region of Interest Overall Presence	Percentage Percentage
Hoescht Concentration	Amount of total DNA	ng/mL
Glycosaminoglycan (GAG)	Total GAG/Total DNA Total GAG/Dry Weight	µg mg

Table 2: *Table summarizing collected outcome measurements. Ultrasound and magnetic resonance evaluations performed on days 0, 14, 60, 90 and 214. Post-mortem evaluation (day 214) consisted of histologic, biochemical and immunohistochemical analysis.*

The tendon lobe and lesion size were determined by first using the free-hand region of interest (ROI) tool on each sequence (PD, T2, STIR) to obtain a cross-sectional area (CSA) measurement in cm^2. The measured CSA for each limb was then multiplied by the sum of the slice thickness and slice gap to give resultant mean tendon lobe and mean lesion volume measurements, respectively. The cumulative volume of the affected tendon lobe and lesion were then determined by summing the calculated volume of each slice.

Quantitative tendon lobe and lesion signal intensity measurements were determined by using the uniformly sized ellipse ROI tool to determine each region's grey value ratio. The resultant grey value ratio of each slice was then averaged and divided by the measured intensity of the middle phalangeal cortex to determine the mean intensities of the affected tendon lobe and lesion. All images were calibrated using the axial palmar cortex of the middle phalanx to account for differences in signal to noise ratios on different MR examinations.

Ultrasonographic image acquisition and analysis

Ultrasonographic examination of the DDFT within the pastern of all horses was performed by a board-certified veterinary radiologist (GDR) and radiology resident experienced in equine ultrasound (EWB) at all imaging time points using a 12.5 MHz 38mm linear array transducer (Biosound MyLab 70, Esaote North America Inc., Indianapolis, IN) in a weight-bearing position.

All ultrasound images were analyzed on a diagnostic imaging viewing station monitor. All images were randomized for evaluation and analyzed by a single reviewer (EWB) who was blinded to treatment groups. Quantitative measurements for four ultrasound outcome parameters were made from obtained images: 1) tendon CSA; 2) lesion CSA; 3) lesion echogenicity and 4) longitudinal fiber pattern (Table 2). Specifically, cross-sectional area measurements were made for both the lesions and tendons 3 cm proximal to the pastern joint, at the level of the pastern joint and 2 cm distal to the pastern joint on transverse images using the free-hand ROI tool. Echogenicity of the lesions was assessed on transverse images using a 1 - 4 ordinal scale: (1 = isoechoic compared to unaffected adjacent tendon; 2 = mildly hypoechoic compared to unaffected adjacent tendon; 3 = moderately hypoechoic compared to unaffected adjacent tendon; 4 = anechoic compared to unaffected adjacent tendon). Lastly, longitudinal fiber pattern was assessed on longitudinal axis images using an ordinal scale of 1 - 4: (1 = 0 - 25% heterogenous longitudinal fiber pattern, 2 = 26 - 50% heterogenous longitudinal fiber pattern, 3 = 51 - 75% heterogenous longitudinal fiber pattern, 4 = 76 - 100% heterogenous longitudinal fiber pattern).

Tissue harvest

Following the 214-day imaging evaluation, all horses were sedated with 400 mg of xylazine hydrochloride IV prior to euthanasia. Horses were then euthanized using 120 mL of sodium pentobarbital administered IV as a rapid bolus in accordance with the AVMA guidelines on euthanasia. At post-mortem, a longitudinal incision was made to remove the skin and subcutaneous tissue overlying the forelimb DDFTs from the level of the fetlock to the coronet band. All DDFTs were visually evaluated, gross observations were recorded and limbs were photographed. To ensure that the center of lesion location remained consistent for all aspects of analysis, a suture was placed at the site of the most grossly injured area of the DDFT. The location of this suture and its distance relative to the fetlock joint was then recorded and used as the center of evaluation for future multi-modality analysis.

The forelimbs of all horses were then disarticulated at the level of the middle carpal joint and the DDFTs were carefully harvested from the fetlock region to the level of the coronet band using sharp dissection and Brown-Adson tissue forceps. Care was taken to minimize tissue handling when possible. Tendon samples were then immediately processed for histologic, immunohistochemical (IHC) and biochemical analysis.

Specimen preparation

Following tissue harvest, the site of the previously placed suture (central portion of the lesion) was transected and sections of the affected portion of the tendon were then divided equally into sections for histologic, immunohistochemical and biochemical examination. Samples for histologic examination were fixed in 10% neutral buffered formalin solution for 48 hours, then stored at 4°C in sterile phosphate buffered saline (PBS) until processing. Samples for immunohistochemical analysis were covered with Optimal Cutting Temperature Compound (American Master*Tech Scientific Incorporated, Lodi, CA), snap-frozen in liquid nitrogen and then stored at -80°C until processing. Samples obtained for biochemical analysis were snap-frozen in liquid nitrogen until processing.

Histologic, immunohistochemical and biochemical preparation

Formalin fixed tissue sections were dehydrated, cleared in xylene, embedded in paraffin, sectioned (5 μm thick) and mounted on microscope slides. Tissue morphology was examined with hematoxylin and eosin (H&E) staining and collagen crimping was evaluated using picosirius red staining and polarized light microscopy. Scoring for cellular shape, cellular density, hemorrhage, neovascularization, amount of inflammatory cellular infiltrate, linearity of collagen fibers, uniformity and crimping of collagen fibers was assessed using a previously described ordinal scale (Table 2, 0 = normal; 4 = severe) [9,10]. A total histologic score was calculated by summing the individual scores from each category.

Immunohistochemical analysis was used to investigate the distribution of collagen type I and III proteins in two tissue sections using a manner like that previously described [9]. Briefly, fresh frozen tissues were embedded in OCT medium, sectioned (8 μm thick) and probed with antibodies for collagen type I (Accurate Chemical & Scientific Company, Westbury, NY) and collagen type III (BioGenex, Fremont, CA). Blocking serum that was protein matched to the primary antibody protein concentration was used for the negative control sections (Donkey antimouse HRP secondary, Jackson ImmunoResearch, West Grove, PA and Negative control mouse serum, Jackson ImmunoResearch, West Grove, PA). For detection, all samples were treated with a horseradish peroxidase conjugated secondary antibody (Jackson ImmunoResearch Laboratories, West Grove, PA) followed by detection using streptavidin conjugated peroxidase to catalyze color production from the chromagen diaminobenzidine tetrachloride. Sections were then counter stained with Harris hematoxylin and immunoreactivity was graded on an ordinal scale of 1 to 4 as previously described (Table 2) [9,10].

Glycosaminoglycan and DNA were quantified in frozen tendon specimens from two tissue sections by lyophilizing the specimen and digesting with 8U papain/mL using the protocol previously described [10]. A spectrophotometric dimethylmethylene blue dye binding (DMMB) assay quantified the glycosaminoglycan content following digestion for 18 hours at 60°C in .5% papain. DNA quantification was assessed using the Hoescht assay as previously described [11]. Soluble collagen levels were measured using the sirius red-dye binding method (Sircol Soluble Collagen Kit, Bicolor LTD, County Antrim, UK) in a manner similar to that previously reported [10]. All values were normalized to original tissue dry weight and DNA content. All tissue analysis was performed by one of the authors (DDF) with advanced training and experience in histologic and biochemical processing and assessment. This author was blinded to treatment groups for all tissue analyses.

Statistical analyses

Statistical analysis was performed using commercial software (SAS v9.4; SAS Institute, Cary, NC; R 3.0.2 sciplot package 1.1-0, R Foundation for Statistical Computing, Vienna, Austria; RStudio 0.98.932, RStudio, Inc., Boston, MA). To investigate the relationships between treatment and response variables of post-mortem tissue analysis, a generalized linear mixed model analysis of variance (ANOVA) with repeated measures was fit. To account for the design of data collection, the model included fixed effects of treatment, age, and date and the horse as a random effect. Diagnostic plots were used to assess assumptions of equal variance and normality. Based on these plots, assumptions were met. Significance for all tests was set at $P \leq 0.05$.

Results

Magnetic resonance imaging evaluation

At 60 days post-treatment, lesion volume was significantly larger in MSC-treated limbs on both PD and T2-weighted sequences (Figure 2A and 2B) (P = 0.01, 95% Confidence Interval (CI): [-0.49 - -0.07], P = 0.02, CI: [-0.47 - -0.041], respectively). Similarly, tendon lobe volume of MSC-treated limbs was significantly larger on the T2-weighted sequence at 60 days than controls (Figure 3) (P = 0.03, CI: [-1.01 - -0.06]). No further differences in size or signal intensity (lesion or tendon lobe) were appreciated between treatment groups.

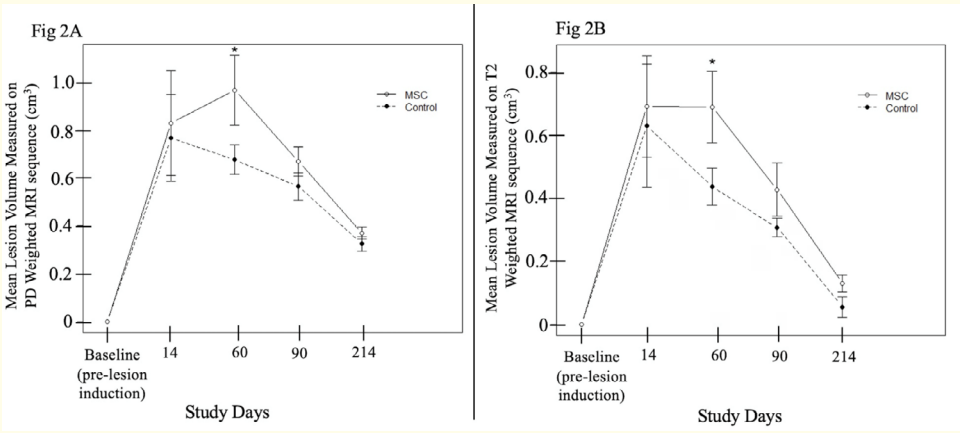

Figure 2: *Mean lesion volume measured on 2A) proton density (PD) weighted and 2B) T2 weighted turbo spin echo (TSE) magnetic resonance imaging (MRI) sequences in mesenchymal stem cell (MSC) treated tendons and non-injected controls across study time points. Standard error values are also presented. *indicates a statistically significant difference (P < 0.05).*

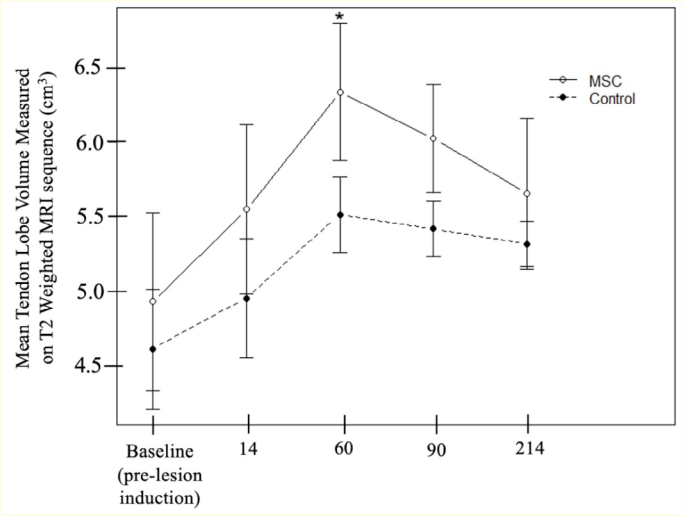

Figure 3: *Mean tendon lobe volume measured on T2 weighted turbo spin echo (TSE) magnetic resonance imaging (MRI) sequence in MSC treated tendons and non-injected controls across study time points. Standard error values are also presented. * indicates a statistically significant difference (P < 0.05).*

Ultrasonographic evaluation

Lesion CSA measurements were significantly larger in the MSC-treated limbs at 60 (P = 0.002, CI: [-11.3 - -2.6]) and 90 (P = 0.04, CI: [-8.9 - -0.2]) days post treatment (Figure 4). No significant differences between treatment groups in lesion CSA at days 14 or 214 were appreciated. No significant differences in tendon CSA measurements, longitudinal fiber pattern or echogenicity were observed between treatment groups.

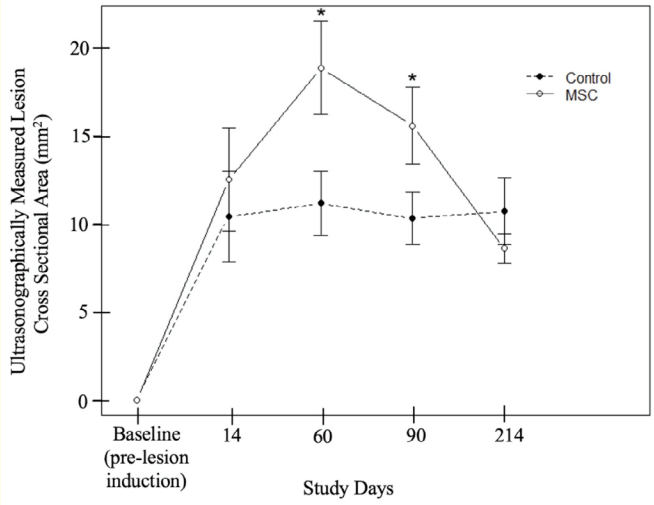

Figure 4: *Mean lesion cross sectional area measured on greyscale ultrasound in mesenchymal stem cell (MSC) treated tendons and non-injected controls across study time points. Standard error values are also presented. * indicates a statistically significant difference (P < 0.05).*

Histologic, immunohistochemical and biochemical outcomes

The amount of inflammatory cellular infiltrate was significantly lower in MSC-treated tendons (P = 0.05, CI: [0.003 - 0.7]). Glycosaminoglycan content (normalized for DNA content) was also significantly lower in MSC-treated tendons (P = 0.002, CI: [2.03 - 5.7]). Further statistically significant relationships between treatment group and histologic, biochemical or immunohistochemical outcomes were not observed. Results are presented in table 3.

Histologic Analysis	MSC-treated Tendons	Non-injected Control Tendons	Standard Error	P value
Cell Shape	1.86	1.68	0.24	0.60
Cell Density	1.59	1.34	0.30	0.50
Hemorrhage	0.32	-0.01	0.15	0.05
Neovascularization	0.58	0.64	0.20	0.80
Inflammatory Cellular Infiltrate	0.02	0.39	0.19	0.05*
Total H&E Score	4.38	4.05	0.84	0.74
Percent Abnormal Tissue	48.33	49.64	8.12	0.91
Collagen Linearity	2.21	1.69	0.24	0.14
Collagen Uniformity	2.52	1.92	0.26	0.12
Collagen Crimping	1.05	0.77	0.26	0.47
Fascia Thickness	2.14	1.71	0.22	0.18
Total Picosirius	7.93	6.10	0.74	0.10
Toluidine Blue	1.91	1.91	0.74	1.00
Total Histologic Score	19.96	17.01	1.35	0.14

Biochemical Analysis	MSC	Control	Standard Error	P value
µg GAG/mg Tissue	16.00	19.37	1.69	0.15
µg DNA/mg Tissue	2.62	2.03	0.32	0.14
µg GAG/µg DNA	6.45	9.97	0.72	0.002*
µg Soluble Collagen/mg Tissue	180.47	198.63	31.92	0.70
Immunohistochemical Analysis	**MSC**	**Control**	**Standard Error**	**P value**
Collagen I, adjacent tendon	74.65	73.55	9.30 (MSC) 10.1670 (Control)	0.93
Collagen I, lesion	77.02	79.38	8.39 (MSC) 9.32 (Control)	0.85
Collagen III, adjacent tendon	61.35	44.18	10.25 (MSC) 11.24 (Control)	0.25
Collagen III, lesion	71.94	89.13	10.81 (MSC) 11.58 (Control)	0.21

Table 3: *Table summarizing mean histologic, immunohistologic and biochemical scores of mesenchymal stem cell (MSC) treated tendons compared to non-injected controls. Standard error values are also presented. Asterisk indicates significant P value.*

Discussion

The objective of this study was to evaluate the effects of intra-lesional MSCs compared to untreated controls in a collagenase model of intrathecal DDF tendinopathy. The results of this study demonstrate that the use of MSCs significantly lessened the amount of inflammatory cellular infiltrate and glycosaminoglycan content in collagenase induced DDF tendinopathy. Magnetic resonance imaging comparison between MSC-treated tendons and non-injected controls revealed that lesion and tendon lobe volumes were larger in MSC-treated tendons at 60 days post lesion induction. Similarly, ultrasonographically measured lesion volumes were larger in MSC-treated tendons at 60- and 90-days post lesion induction. Further differences in imaging characteristics at other evaluated time points were not appreciated.

The therapeutic use of MSCs in tendinopathic healing has been previously investigated in naturally occurring SDFT injury [4-5,12] and experimental models of tendinopathy [6,7,13], but has yielded a spectrum of results. Clinical usage of MSCs in SDF tendinopathy is supported by approximately 30% reduced re-injury rates in National Hunt horses [5], the ability to return to previous level of work [14] and beneficial effects at the cellular level as evidenced through improved histologic scoring, lower cellularity and reduced glycosaminoglycan content [4]. Elevated levels of glycosaminoglycans have been directly linked to decreased biomechanical strength [15,16] and mitigation of this scar tissue protein represents a promising therapeutic target for improved tendon healing [4, 17,18]. Similarly, collagenase models of SDFT injury have documented improved histologic scores [7], fiber orientation [19] and extracellular matrix ratios of collagen types I/III following intra-lesional injections of MSCs [19].

The results reported herein of 130% less inflammatory cellular infiltrate and 42% less glycosaminoglycan deposition of MSC-treated limbs with collagenase-induced intrathecal DDFT lesions (Table 3) are encouraging and consistent with reported SDFT responses to MSC treatment [4]. Histologic grades for overall inflammatory cellular infiltrate were significantly lower in MSC-treated tendons compared to controls (Table 3), but scores in general were low for both groups, which may reflect study duration, or the model of tendon injury used.

Representative histologic images in both a control and MSC-treated limb are presented in figure 5. This study specifically used a longer investigative duration (214 days) compared to other reported studies [7,19]. The comparable results described herein suggest that similar findings reported in studies of shorter duration may have support for longer term differences. It is the authors' interpretation that 10 - 20% reductions in inflammatory cellular infiltrate and glycosaminoglycan are clinically significant for improved tendon healing, but the study reported herein did not evaluate clinical parameters so direct inferences cannot be made. Given that the results reported here exceed those reductions in a more long-term investigation and in absence of negative effects, the role of MSCs in improving intrathecal tendon healing at the cellular level through less inflammatory infiltrate and glycosaminoglycan warrants further investigation.

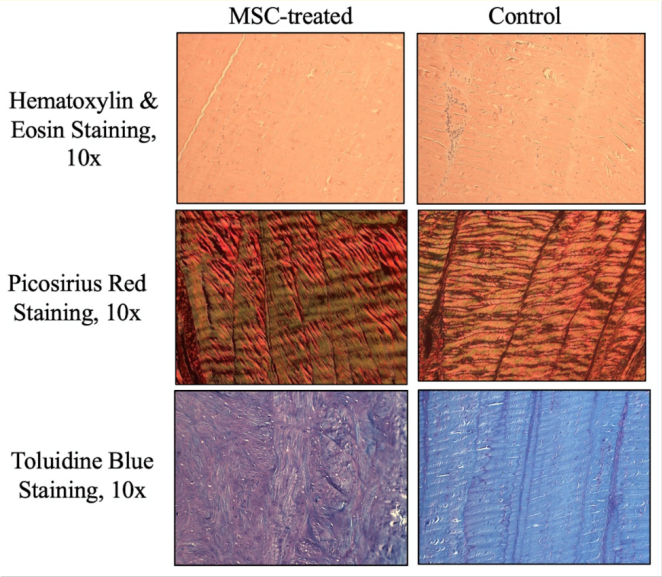

Figure 5: *Representative histologic images of collagenase-induced deep digital flexor (DDF) tendinopathy of untreated (control) limbs and limbs treated with intra-lesional mesenchymal stem cells (MSC-treated). Analysis revealed the amount of inflammatory infiltrate was significantly lower in MSC-treated tendons (P = .05). Further significant differences for other evaluated histologic outcomes were not appreciated.*

Interestingly, differences in collagen expression or cellular morphology were not simultaneously noted as previously described for extrathecal SDFT responses [7]. Intrathecal DDFT responses to injury that differ from those of extrathecal SDFT tendons may explain why other statistically significant cellular differences (cellular morphology, collagen types I/III, etc.) were not appreciated in the present study. Another potential explanation may be related to tendinopathic responses to collagenase-induced injury that differ from other models of disease and naturally occurring injury. Additionally, the distal limb DDFT is quite unique in its structural and biomechanical morphologies as it courses proximally to distally. In a histopathologic study investigating lesions of the DDFT in the digit, a significant portion of core lesions extended from the proximal aspect of the navicular bursa into the proximal aspect of the pastern, occupying the digital flexor tendon sheath and demonstrating proteoglycan deposition [20]. Similarly, in a study of naturally occurring DDFT injury at the level of the navicular bone, investigators found increased levels of proteoglycan, suggesting an alteration in DDFT matrix composition may be an indicator of degenerative change [21]. With such few reports documenting more proximal histopathologic responses, however, the frequency of comprehensive degenerative changes in intrathecal tendon injury is still largely unknown [17] and difficult to extrapolate to experimentally induced tendon injury.

Intrathecal DDF tendinopathy is typically diagnosed using grey-scale ultrasonography or MRI. The incorporation of longitudinal imaging assessments (Figure 6) in the present study was utilized to not only visualize the collagenase model of tendinopathy, but also to document imaging differences that may exist between MSC-treated tendons and non-injected controls. To the authors' surprise, very few imaging differences were found statistically significant. Magnetic resonance imaging comparison between MSC-treated tendons and non-injected controls revealed that at 60 days post-treatment, lesion volume was significantly larger in MSC-treated limbs on both PD and T2-weighted sequences (Figure 2A and 2B). This finding is likely the result of the volume injected (0.2 mL injected into five sites for a total volume of 1mL) into MSC-treated lesions of a relatively thin tendon that was not similarly introduced into control lesions, and its relevance should be interpreted with caution. Another potential explanation involves a cellular response elicited by the presence of MSCs that may be related to increased cellular activity related to healing [22,23]. This hypothesis is supported by the fact that hyperintensity manifested as increased signal intensity on PD and T2-weighted sequences can indicate the presence of edema, increased cellularity or even hemorrhage [24], which may explain why MSC-treated lesions were largest at this timepoint. A further explanation could be introduction of the needle itself to deliver the MSCs under ultrasound guidance.

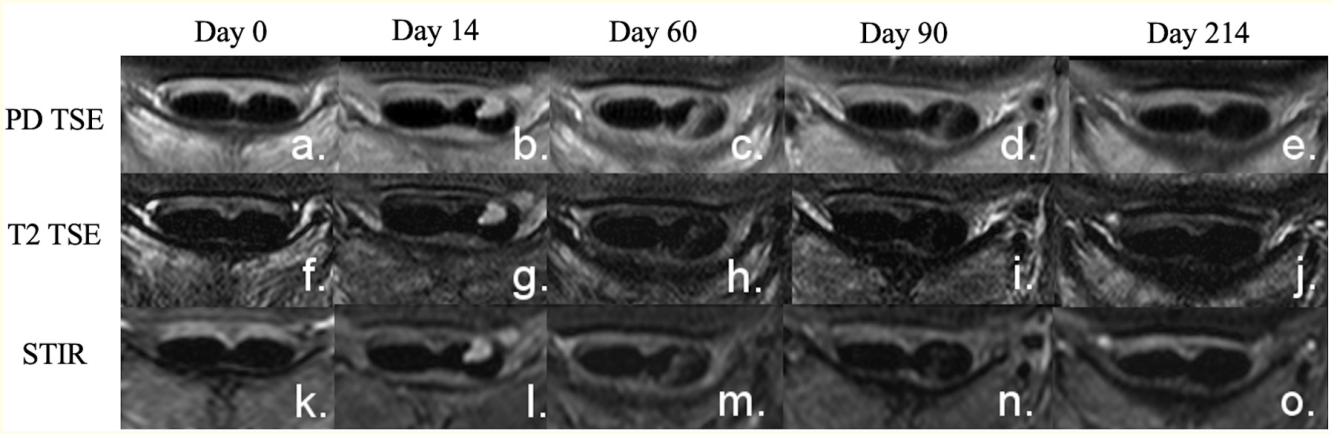

Figure 6: *Longitudinal magnetic resonance (MR) images of collagenase-induced tendinopathy of the deep digital flexor tendon at the level of the proximal interphalangeal joint on study days 0, 14, 60, 90 and 214. Depicted MRI sequences include proton-density turbo spin echo (PD TSE, rows a-e), T2-weighted turbo spin echo (T2 TSE, rows f-j) and short τ inversion recovery (STIR, rows k-o). All images are from an un-injected control limb from the same horse at all evaluated study time points.*

Also interesting was the finding that tendon lobe volume of MSC-treated limbs was significantly larger on the T2-weighted sequence at 60 days compared to non-injected controls (Figure 3). This observation may be due to injection volume differences, the phase of tissue healing at 60 days or the fact that MSC-treated tendon lobe volumes were larger prior to lesion induction or MSC injection, although not statistically significant (Figure 3). It is possible that inherent size differences appreciated initially contributed to this finding, or that ongoing healing responses resulted in global enlargement of the tendon lobe. Without correlative histopathologic analysis at the 60-day timepoint, it is difficult to fully conclude the relevance of this finding.

Lastly, ultrasonographically assessed lesion CSA measurements were significantly larger in the MSC-treated limbs at 60- and 90-days post treatment (Figure 4), while no significant differences in ultrasonographic tendon CSA measurements, longitudinal fiber pattern or

echogenicity were observed between treatment groups. These findings were similar in nature to MRI lesion assessment at 60 days, and in turn are likely a reflection of volume injected into MSC-treated tendons or tissue reaction associated with healing itself or needle introduction. Lack of significant differences in the other ultrasound parameters may reflect sensitivity of the modality itself, inherent variation in assessment or an inability for grey-scale ultrasound characteristics to reflect ongoing physiologic events.

Study limitations the authors would like to acknowledge include inherent variability in the experimental induction of tendinopathy using collagenase in a small sample population. While no model has been universally agreed upon to exactly replicate clinical disease, this study is a pilot investigation that standardized intrathecal DDFT lesions to assess the therapeutic value of MSCs and allow reasonable comparison to other published studies. The MSCs utilized herein were delivered via intra-lesional injection, but it was not an objective of this study to document their retention within the enzymatically damaged site. Even with MSCs being locally retained at less than 10%, proximity or potency influences have demonstrated therapeutic value [7,25]. Furthermore, one forelimb of each horse was treated with MSCs, while the contralateral limb of the same horse received no control injection. Separating the treatment groups by horse instead of limb would have eliminated any systemic MSC-effects, despite no relationship having been documented to date. The authors realize that trafficking of cytokines and other paracrine factors likely occurs but controlling for horse response variability was prioritized more than systemic effects in consideration of this study design. Additionally, injecting control lesions with 1 mL of saline would have eliminated any healing responses associated with the volume utilized, but not allowed the more clinically relevant comparison for when lesions are not injected with anything (untreated). Not utilizing a 1mL saline control allowed the MSC treatment to be compared to truly untreated tendons, which is often the most common clinical scenario. It does, however, set up an inherent study bias and increases the volume of tendon disruption that is not controlled for by study design. It is also not possible to discern therapeutic effects of MSCs from any benefit of the introduction of the needle itself. Different results may also have been appreciated if a different post-injection exercise regimen had been utilized or if imaging and/or tissue evaluations had been performed at different study time points. Lastly, the preferential timing, dosage and method of delivery for MSCs within the spectrum of tendon lesions remains unknown, so it is possible that differences may have been appreciated had a different protocol or study timeline been used. The authors utilized MSCs as described herein to most closely mimic current clinical usage. Biomechanical testing may also have revealed functional strength differences that may be extrapolated to clinical differences. Further studies investigating these tissue-specific effects under various modes of delivery and clinical outcome will be useful.

Conclusion

In conclusion, the results of this study demonstrate that the use of MSCs significantly lessened the amount of inflammatory cellular infiltrate and glycosaminoglycan content in collagenase induced DDF tendinopathy. Minimal differences in ultrasonographic or MRI imaging characteristics were appreciated, leading authors to speculate that physiologic effects of MSCs may not manifest as imaging-apparent differences. Lesion and tendon lobe size differences appreciated on imaging analysis were likely due to injection volume differences. Further investigation into the use of MSCs to mitigate formation of the biomechanically inferior scar tissue protein glycosaminoglycan is warranted.

Conflicts of Interest

Dr. Frisbie and Dr. Schneider have stock in Advanced Regenerative Therapies.

Funding Sources

Funding for this project was provided by the Robert B. McEachern Distinguished Professor in Equine Medicine Fund and the Washington State University Orthopedic Research Fund.

Bibliography

1. Dyson S and Murray R. "Magnetic resonance imaging evaluation of 264 horses with foot pain: the podotrochlear apparatus, deep digital flexor tendon and collateral ligaments of the distal interphalangeal joint". *Equine Veterinary Journal* 39 (2007): 340-343.

2. Lutter J., *et al*. "Medical treatment of horses with deep digital flexor tendon injuries diagnosed with high-field-strength magnetic resonance imaging: 118 cases (2000-2010)". *Journal of the American Veterinary Medical Association* 247.11 (2015): 1309-1318.

3. Cillan-Garcia E., *et al*. "Deep digital flexor tendon injury within the hoof capsule; does lesion type or location predict prognosis?" *Veterinary Record* (2013).

4. Smith R., *et al*. "Beneficial effects of autologous bone marrow-derived mesenchymal stem cells in naturally occurring tendinopathy". *PLOS one* 8.9 (2013): e75697.

5. Godwin E., *et al*. "Implantation of bone marrow-derived mesenchymal stem cells demonstrates improved outcome in horses with overstain injury of the superficial digital flexor tendon". *Equine Veterinary Journal* 44 (2012): 25-32.

6. Ahrberg A., *et al*. "Effects of mesenchymal stromal cells versus serum on tendon healing in a controlled experimental trial in an equine model". *BMCM Disorders* 19 (2018): 230.

7. Schnabel L., *et al*. "Mesenchymal stem cells and insulin-like growth factor-I gene-enhanced mesenchymal stem cells improve structural aspects of healing in equine flexor digitorum superficialis tendons". *Journal of Orthopaedic Research* 27 (2009): 1392-1398.

8. Lake S., *et al*. "Animal models of tendinopathy". *Disability and Rehabilitation* 30 (2008): 20-22.

9. Nixon A., *et al*. "Effect of adipose-derived nucleated cell fractions on tendon repair in horses with collagenase-induced tendinitis". *American Journal of Veterinary Research* 69 (2008): 928-937.

10. Marsh C., *et al*. "Evaluation of bone marrow-derived mesenchymal stem cells as a treatment for collagenase-induced desmitis of the proximal suspensory ligament in horses". Proc. Ann. Conv. Am. Assoc. Eq. Pract. 58 (2012): 54-55.

11. Kim YJ., *et al*. "Fluorometric assay of DNA in cartilage explants using Hoescht 33258". *Analytical Biochemistry* 174 (1988): 168-176.

12. Smith R. "Mesenchymal stem cell therapy for equine tendinopathy". *Disability and Rehabilitation* 30.20-22 (2008): 1752-1758.

13. Carvalho A., *et al*. "Evaluation of mesenchymal stem cell migration after equine tendonitis therapy". *Journal of Equine Veterinary Science* 46 (2014): 635-638.

14. Renzi S., *et al*. "Autologous bone marrow mesenchymal stromal cells for regeneration of injured equine ligaments and tendons: a clinical report". *Research in Veterinary Science* 95 (2013): 272-277.

15. Choi R., *et al*. "Chondroitin sulphate glycosaminoglycans contribute to widespread inferior biomechanics in tendon after focal injury". *The Journal of Biomechanics* 49 (2016): 2694-2701.

16. Bell R., *et al*. "Controlled treadmill exercise eliminates chondroid deposits and restores tensile properties in a new murine tendinopathy model". *The Journal of Biomechanics* 46.3 (2013): 498-505.

17. Smith R and McIlwraith W. "Advances in the understanding of tendinopathies: a report on the second Havemeyer workshop on equine tendon disease". *Journal of Equine Veterinary Science* 46 (2014): 4-9.

18. Ryan C., *et al*. "Glycosaminoglycans in tendon physiology, pathophysiology and therapy". *Bioconjugate Chemistry* 26 (2015): 1237-1251.

19. Crovace A., *et al*. "Histological and immunohistochemical evaluation of autologous cultured bone marrow mesenchymal stem cells and bone marrow mononucleated cells in collagenase-induced tendinitis of equine superficial digital flexor tendon". *Veterinary Medicine International* (2010).

20. Blunden A., *et al*. "Lesions of the deep digital flexor tendon in the digit: a correlative MRI and postmortem study in control and lame horses". *Journal of Equine Veterinary Science* 41.1 (2009): 25-33.

21. Beck S., *et al*. "Are matrix and vascular changes involved in the pathogenesis of deep digital flexor tendon injury in the horse?" *Journal of Veterinary Science* 189 (2011): 289-295.

22. Shojaee A and Parham A. "Strategies of tenogenic differentiation of equine stem cells for tendon repair: current status and challenges". *Stem Cell Research and Therapy* 10 (2019): 181.

23. Burk J., *et al*. "Growth and differentiation characteristics of equine mesenchymal stromal cells derived from different sources". *Journal of Veterinary Science* 195 (2013): 98-106.

24. Winter MD. "The basics of musculoskeletal magnetic resonance imaging". *Veterinary Clinics: Equine* 28 (2012): 599-616.

25. Scharf A., *et al*. "MRI-based assessment of intralesional delivery of bone marrow-derived mesenchymal stem cells in a model of equine tendonitis". *Stem Cells International* (2016).

Volume 12 Issue 7 July 2021